

Kinetic analysis of fluorescein and dihydrofluorescein effluxes in tumour cells expressing the multidrug resistance protein, MRP1

Chantarawan Saengkhae, Chatchanok Loetchutinat, Arlette Garnier-Suillerot*

*Laboratoire de Physicochimie Biomoléculaire et Cellulaire (LPBC-CSSB) UMR CNRS 7033, Université Paris Nord,
74 rue Marcel Cachin, 93017 Bobigny, France*

Received 19 September 2002; accepted 29 November 2002

Abstract

Multidrug resistance (MDR) in tumour cells is often caused by the overexpression of two transporters the P-glycoprotein (P-gp) and the multidrug resistance-associated protein (MRP1) which actively pump out multiple chemically unrelated substrates across the plasma membrane. A clear distinction in the mechanism of translocation of substrates by MRP1 or P-gp is indicated by the finding that, in most of cases, the MRP1-mediated transport of substrates is inhibited by depletion of intracellular glutathione (GSH), which has no effect on their P-gp-mediated transport. The aim of the present study was to quantitatively characterise the transport of anionic compounds dihydrofluorescein and fluorescein (FLU). We took advantage of the intrinsic fluorescence of FLU and performed a flow cytometric analysis of dye accumulation in the wild-type drug sensitive GLC4 that do not express MRP1 and its MDR subline which display high level of MRP1. The measurements were made in real time using intact cells. The kinetics parameters, $k_a = V_M/K_m$, which is a measure of the efficiency of the transporter-mediated efflux of a substrate, was very similar for the two FLU analogues. They were highly comparable with values for k_a of other negatively charged substrates, such as GSH and calcein. The active efflux of both FLU derivatives was inhibited by GSH depletion.

© 2003 Elsevier Science Inc. All rights reserved.

Keywords: Multidrug resistance; MRP1; Fluorescein; Kinetic parameters

1. Introduction

The MRP1-encoded multidrug resistance protein (MRP1) and the MDR1-encoded P-gp are both plasma membrane transporters thought to be responsible in part for the resistance of tumour cells to multiple chemically unrelated drugs (MDR) [1–3]. Both proteins belong to the superfamily of the so-called ATP binding cassette transport proteins or traffic ATPases [4], which are known to be dependent on ATP hydrolysis for the translocation of substrate across

membranes. The substrate specificity of both transporter proteins is partly overlapping and for instance, anticancer drugs, such as anthracyclines, vinca alkaloids and etoposide, are substrates of both transporters. By pumping these agents out of the tumour cells, MRP1 causes reduced intracellular accumulation of drugs, leading to resistance. MRP1 has been described as an ATP-dependent export GS-X pump for the endogenous GSH conjugate leukotriene C4 and structurally related anionic amphiphilic conjugates [5,6], whereas P-gp seems to prefer neutral or positively charged molecules [7]. A clear distinction in the mechanism of translocation of these types of substrates by MRP1 or P-gp is indicated by the finding that their MRP1-mediated transport is inhibited by depletion of intracellular GSH which has no effect on their P-gp-mediated transport [8,9].

In any case, little is known on the relative pumping efficiency by MRP1 of the different types of substrates and in particular about the mechanism by which GSH facilitates transport of some compounds. The proposal that drug efflux by MRP1 might occur after conjugation with GSH has been questioned [10] and many people are now in

* Corresponding author. Tel.: +33-1-48-38-77-48;
fax: +33-1-48-38-77-77.

E-mail address: garnier@lpbc.jussieu.fr (A. Garnier-Suillerot).

Abbreviations: MDR, multidrug resistance; MRP1, multidrug resistance-associated protein; P-gp, P-glycoprotein; HRP, horse raddish peroxidase; GSH, glutathione; DHF-DA, dihydrofluorescein diacetate; FLU, fluorescein; DHF, dihydrofluorescein; BSO, L-buthionine-(S,R) sulfoximine; PAK-104P, 2-[4-(diphenylmethyl)-1-piperazinyl]ethyl-5-(trans-4,6-dimethyl-1,3,2-dioxaphosphorinan-2-yl)-2,6-dimethyl-4-(3-nitrophenyl)-3-pyridine-carboxylate P oxide; MK571, 3-([3-(2-[7-chloro-2-quinolinyl]ethenyl)phenyl]-(3-dimethylamino-3-oxopropyl)-thio)-methylthio)propanoic acid; C_i , concentration of free intracellular FLU (or DHF).

favour of a co-transport mechanism involving GSH [11–13]. In the context of our research on the mechanisms of drugs active efflux in resistant cells, we have undertaken a kinetic approach to determine the relative pumping efficiency of two chemically related anionic compounds, FLU and dihydrofluorescein (DHF). Small cell lung cancer, GLC4 and GLC4/ADR, which overexpress MRP1, have been used. We have determined quantitative parameters for the active efflux of both compounds and compared them to the values obtained under similar conditions for other substrates either anionic or neutral or cationic. Results from this study show that both FLU and DHF are actively pumped out by MRP1 and that this depends on the presence of GSH. In addition, the active parameter values (V_M/K_m) are very close to those observed for MRP1-mediated efflux of GSH and of calcein which are also anionic substrates [14,15]. This work represents the first report, using intact cells, of real-time measurements of the rate of FLU transport.

2. Materials and methods

2.1. Cell culture

GLC4 and MRP1-expressing GLC4/ADR cells [16] were cultured in RPMI 1640 (Sigma Chemical Co) medium supplemented with 10% foetal calf serum (Biomed) at 37° in a humidified incubator with 5% CO₂. The resistant GLC4/ADR cells were cultured with 1.2 µM doxorubicin until 1–4 weeks before the experiments. Cell cultures used for experiments were split 1:2, 1 day before use in order to assure logarithmic growth. Cells (10⁶/mL; 2 mL per cuvette) were energy depleted via preincubation for 30 min in HEPES buffer with sodium azide but without glucose.

2.2. Drugs and chemicals

Dihydrofluorescein diacetate (DHF-DA) was from Molecular Probes. It was dissolved in DMSO. DHF was prepared by basic hydrolysis of DHF-DA. Stock solutions were prepared just before use. 2-[4-(Diphenylmethyl)-1-piperazinyl]ethyl-5-(*trans*-4,6-dimethyl-1,3,2-dioxaphosphorinan-2-yl)-2,6-dimethyl-4-(3-nitrophenyl)-3-pyridinecarboxylate P oxide (PAK-104P) was a gift from Drs. Shudo, Iwasaki and Akiyama (Nissan Chemical Industries Ltd.). 3-([3-(2-[7-Chloro-2-quinolinyl]ethenyl)phenyl]-{(3-dimethylamino-3-oxopropyl)-thio}-methyl]thio)propanoic acid (MK571) was provided by Dr. R.N. Young (Merck-Frosst Centre for Therapeutic Research). Triton X-100 and horse raddish peroxidase (HRP) were from Sigma and were dissolved in water. Reduced GSH, glutathione transferase from equine liver (GSH_T) and L-buthionine-(*S,R*) sulfoximine (BSO) were from Sigma. Monochlorobimane was from Molecular Probes. Before the experiments, the cells were counted, centrifuged and resuspended in HEPES buffer solutions containing 20 mM

HEPES plus 132 mM NaCl, 3.5 mM KCl, 1 mM CaCl₂, 0.5 mM MgCl₂ and 5 mM glucose at pH 7.3. All other reagents were of the highest quality available. Deionized double-distilled water was used throughout the experiments.

2.3. Intracellular GSH measurement

To quantify free GSH inside the cells we have been used monochlorobimane, which itself is non-fluorescent, but forms a fluorescent adduct through conjugation to GSH by glutathione *S*-transferase [17]. Based on this observation, we have recently developed a very rapid and sensitive fluorometric method for GSH measurement [15]. Cells, 2 × 10⁶ suspended in 2 mL of buffer, were disrupted by sonication on ice (3 × 10 s, power 2). The rate of monochlorobimane–GSH formation was monitored after addition of monochlorobimane 100 µM and glutathione *S*-transferase 0.5 U/mL, as described [15]. In the absence of glutathione *S*-transferase, the rate of formation of the fluorescent derivative was very slow. We checked that oxidised GSH did not give rise to any modification of the fluorescence signal.

2.4. GSH depletion

In order to examine the effect of GSH depletion by BSO on FLU derivative efflux, cells were cultured in the presence of 25 µM BSO for about 18 hr.

2.5. Cellular DHF and FLU accumulation

The methodology for the determination of the kinetics of active transport of fluorescent drugs or any fluorescent probe from tumour cells has been used and discussed before for anthracyclines and calcein [14,18–20]. We have now adapted this technique to measure the kinetics of active DHF and FLU transport. Basically, the fluorescence signal (macrospectrofluorescence) is monitored continuously during incubation of the cells with DHF-DA. DHF-DA is a non-fluorescent molecule. It enters by passive diffusion into the cells where it is transformed in DHF by cytoplasmic esterases. DHF, which is also a non-fluorescent molecule, is oxidised by oxidative species to FLU which is fluorescent (Fig. 1). Since DHF-DA and DHF are non-fluorescent molecules, the fluorescence which is measured is always that of the FLU.

The cells were incubated in a quartz cuvette in a suspension of 10⁶ cells/mL in HEPES buffer with 5 mM glucose as indicated. The fluorescence was recorded on a Perkin Elmer LS50B spectrofluorometer at 520 nm (λ_{ex} = 490 nm). To determine intracellular FLU accumulation inside the cells, during the time course of these experiments, aliquots were taken at various interval of time and used as such for flow cytometry measurements (Becton-Dickinson, Facscan). Details of the experimental set-ups are given in the results section.

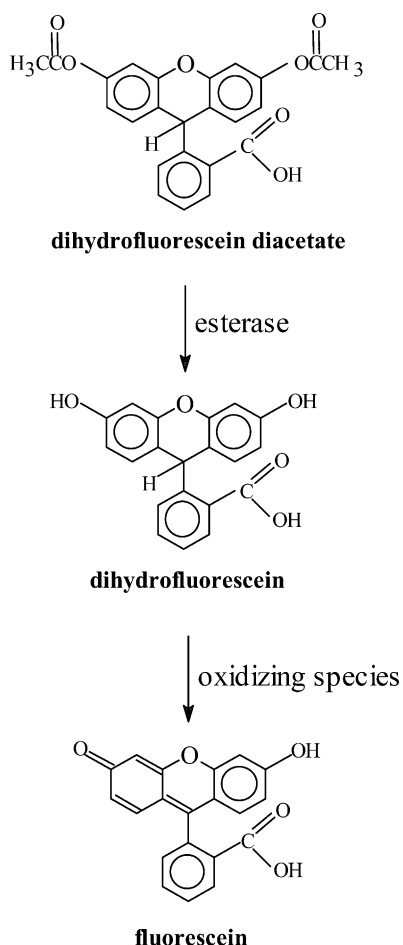


Fig. 1. Structure of dihydrofluorescein diacetate (DHF-DA), dihydrofluorescein (DHF) and fluorescein (FLU).

2.6. Mathematical calculations

In the following V_a will stand for the rate for outward pumping of FLU (or DHF) and \mathcal{C}_i for the concentration of free internal FLU (or DHF). The determination of the kinetic parameters, e.g. the maximum rate (V_M) and the Michaelis constant (K_m), characteristic of the transporter-mediated efflux of any molecule required the measurement of V_a and \mathcal{C}_i . When V_a can be determined for various intracellular free substrate concentrations \mathcal{C}_i , the maximal efflux rate (V_M) and the apparent Michaelis–Menten constant (K_m) can be computed by non-linear regression analysis of transport velocity V_a vs. \mathcal{C}_i assuming that the transport follows the Michaelis equation:

$$V_a = \frac{V_M \times \mathcal{C}_i}{K_m + \mathcal{C}_i} \quad (1)$$

In many cases, the complete curve $V_a = f(\mathcal{C}_i)$ cannot be obtained and, therefore, it is not possible to obtain these two parameters characteristic of a transporter. However, if \mathcal{C}_i is much lower than K_m , Eq. (1) becomes:

$$V_a \approx \frac{V_M}{K_m} \mathcal{C}_i \quad \text{or} \quad V_a = k_a \times \mathcal{C}_i \quad (2)$$

The efficiency of the efflux can then be characterised by calculating k_a , the pump-mediated efflux coefficient for the drug according to the Eq. (2).

3. Results

In order to be able to calculate the kinetic parameters k_a for the active transport of the substrates DHF and FLU, we have performed a series of experiments designed to determine at any time (i) the concentration of free internal FLU and DHF, (ii) the rate constant for outward pumping at limiting FLU and DHF concentrations, i.e. when the substrate concentrations are much lower than K_m and Eq. (2) can be used.

3.1. FLU formation detected using flow cytometry and macrospectrofluorescence

Cells, $10^6/\text{mL}$, were incubated with 20 μM DHF-DA and Fig. 2 shows typical records of the fluorescence intensity as a function of time, using either flow cytometry (F_{cyto}) or spectrofluorometry (F_{macro}). As can be seen, for sensitive cells, F_{cyto} increased during the first hour and then plateaued for at least for one additional hour. However, for GLC4/ADR cells, after a first increase F_{cyto} vanished rapidly indicating that FLU was pumped out. This was corroborated by the observation that when energy-depleted GLC4/ADR cells were used the F_{cyto} signal was similar to that obtained with sensitive cells. The F_{macro} signal increased as a function of time, when either sensitive or resistant cells were used. However, the signal intensity was lower in resistant cells than in sensitive cells, indicating that less FLU was formed and, therefore, that DHF-DA was pumped out by MRP1 as the hydrolysis of DHF-DA to FLU occurred inside the cells only.

3.2. Quantification of DHF and FLU inside the cells

First, we have measured, under our experimental conditions, the molar fluorescence of FLU: F_{FLU} . For this purpose, DHF was prepared by basic hydrolysis of DHF-DA. HRP or HRP + H_2O_2 (the result was the same) was added to a precise concentration of DHF yielding the total conversion of DHF to FLU and macrospectrofluorescence was measured.

Second, we have checked that the quantum yield of FLU was independent of its localisation in the intra- or extracellular medium (see Section 3.3).

Third, sensitive cells, $10^6/\text{mL}$, were incubated with 20 μM DHF-DA and the flow cytometry signal was recorded as a function of time. After 1 hr cells were centrifuged and suspended in a DHF-DA free buffer. The intensity of the signal continue to increase despite the absence of DHF-DA in the extracellular medium. Before centrifugation, the rate for the appearance of the FLU signal depended on

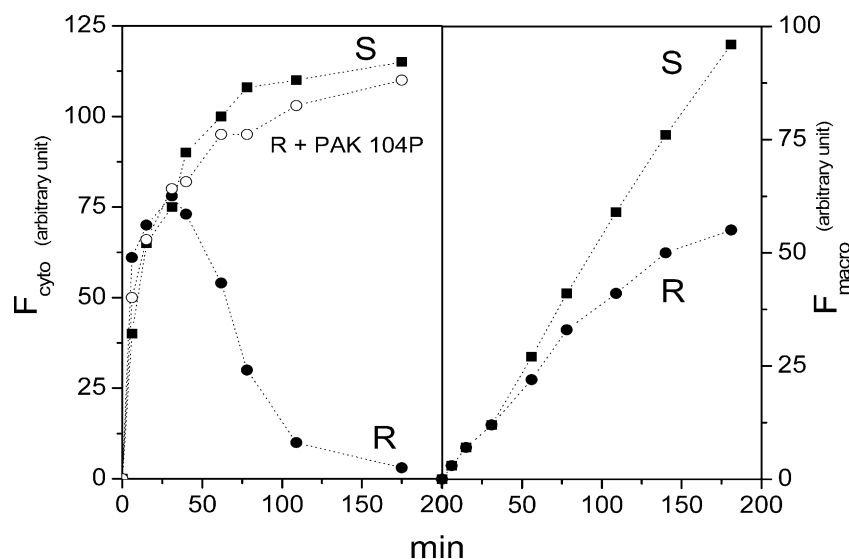


Fig. 2. Uptake of DHF-DA by sensitive and resistant GLC4 cells. Cells, $10^6/\text{mL}$ either sensitive (■), resistant (●) or resistant in the presence of $10\text{ }\mu\text{M}$ PAK-104P (○) were incubated with $20\text{ }\mu\text{M}$ DHF-DA and the fluorescence signals, measured using traditional fluorescence (F_{macro}) and flow cytometry (F_{cyto}), were plotted as a function of the time of incubation. Data points are from a representative experiment.

(1) the rate for the passage of DHF-DA through the plasma membrane, (2) the rate of hydrolysis of DHF-DA to DHF and then (3) the rate of oxidation of DHF to the fluorescent species FLU. The rate of oxidation of DHF to FLU should be proportional to the DHF concentration. The observation that after centrifugation and elimination of DHF-DA in the extracellular medium the rate of FLU signal apparition was the same that before centrifugation, strongly suggested that in both cases the FLU concentration was very similar. Therefore, the limiting step in the formation of FLU was neither the uptake of DHF-DA by cells, nor its hydrolysis to DHF but its intracellular oxidation by oxidising species.

The oxidation of DHF to FLU being slow, we found a way to oxidise it rapidly and completely and measured its intracellular concentration. Cells were incubated for 1 hr with $20\text{ }\mu\text{M}$ DHF-DA. After 1 hr they were centrifuged and suspended in a free DHF-DA buffer. According to the data described earlier, inside the cells DHF and FLU were present. Then H_2O_2 was quickly added which yielded the total and fast conversion of DHF to FLU and the F_{macro} and F_{cyto} signal very quickly recorded (Fig. 3). Under these conditions, the fluorescence signal measured with macrospectrofluorescence (F_{macro}) and with flow cytometry (F_{cyto}) were those of FLU inside the cells. From F_{macro} and the value of the molar fluorescence determined earlier, we calculated $[\text{FLU}]_i$, the intracellular FLU concentration. For that purpose we have assimilated cells to spheres having a mean radius equal to $12\text{--}13\text{ }\mu\text{m}$, as determined with a Coulter counter, and calculated a mean volume equal to 10^{-12} L . Therefore, it was possible to draw a calibration curve by plotting F_{cyto} as a function of F_{macro} (i.e. $[\text{FLU}]_i$) (Fig. 4). It follows that in any experiment, the measure of F_{cyto} yielded $[\text{FLU}]_i$. We have

checked that similar data were obtained with energy-depleted resistant cells indicating that the conversion of DHF to FLU was similar in both the sensitive and resistant cell lines.

As DHF was non-fluorescent, the determination of its intracellular concentration could only be indirect: cells were incubated with DHF-DA, F_{cyto} was measured before the addition of H_2O_2 , yielding $[\text{FLU}]_i$, and after the addition of H_2O_2 . The increase of F_{cyto} yielded the intracellular concentration of DHF which was present inside the cells and had been converted to FLU by H_2O_2 addition.

3.3. Control experiments

After having established the principle of the experiments, as explained earlier, a set of control experiments was performed in order to further validate the use of the experimental model to analyse the transport kinetics of FLU and DHF.

First, a control experiment was done in order to establish that the fluorescence properties of FLU under these conditions are the same inside or outside the cells. Therefore, after 1 hr of cell incubation with DHF-DA, cells were centrifuged and suspended in DHF-DA free buffer and F_{macro} recorded. Then, the plasma membranes were disrupted by sonication and we observed that the fluorescence signal was not significantly modified. This indicates that there are only minor differences in FLU fluorescence in- or outside the cells and that there does not seem to be self-quenching of FLU at the $[\text{FLU}]_i$ which are reached in the intracellular volume (see later). In addition, we examined the GLC4 and GLC4/ADR cells by fluorescence microscopy after loading with DHF-DA. It appeared that in these cells the FLU fluorescence was evenly distributed throughout the

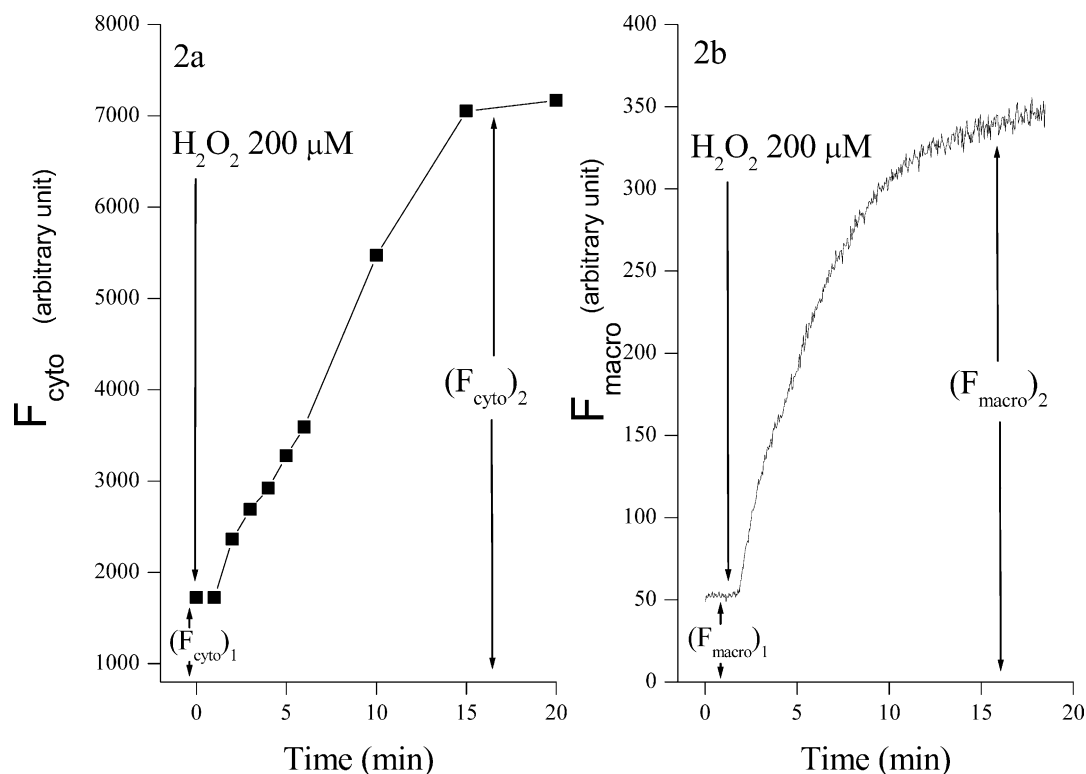


Fig. 3. Oxidation of the intracellular DHF to FLU by addition of H_2O_2 . Sensitive cells ($10^6/\text{mL}$) were incubated with $20 \mu\text{M}$ DHF-DA. After 1 hr cells were centrifuged and suspended in a free DHF-DA buffer. The fluorescence signal measured using traditional fluorescence (F_{macro}) and flow cytometry (F_{cyto}) was recorded as a function of the time of incubation. The fluorescence signals ($F_{\text{cyto}})_1$ and ($F_{\text{macro}})_1$ were due to FLU inside the cells. Then $200 \mu\text{M}$ H_2O_2 was quickly added which yielded the total and fast conversion of the intracellular DHF to FLU. The fluorescence signals ($F_{\text{cyto}})_2$ and ($F_{\text{macro}})_2$ were due to the oxidation of DHF to FLU. Data points are from a representative experiment.

nucleus and cytoplasm. Together these results justify the assumption made for our calculations that the FLU may be regarded as evenly distributed without evidence of self-quenching.

A second control experiment was made with H_2O_2 . The oxidation of DHF to FLU by addition of H_2O_2 to the cells was performed at various concentrations of H_2O_2 and we have checked that it depended on the H_2O_2 concentration

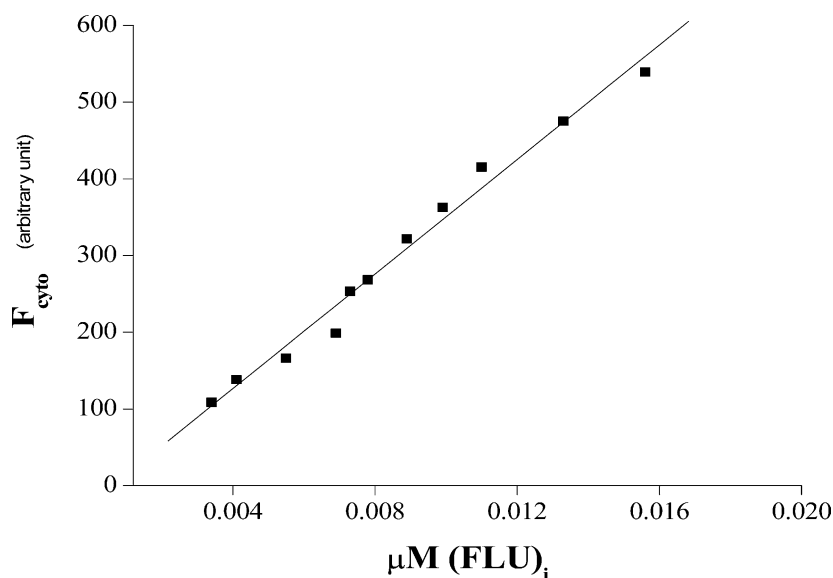


Fig. 4. Flow cytometry and the cytosolic free FLU concentration. The experimental conditions are the same as those in Fig. 3. The signal F_{cyto} recorded after the addition of H_2O_2 has been plotted as a function of $[\text{FLU}]_i$, the intracellular FLU concentration. $[\text{FLU}]_i$ was calculated using the following equation: $[\text{FLU}]_i = (F_{\text{macro}}/F_{\text{FLU}}) \times 10^3$ where F_{FLU} is the molar fluorescence of FLU determined as described earlier and it is taken into account that 10^6 cells/mL are used and that the intracellular volume is $\sim 10^{-12}$ L.

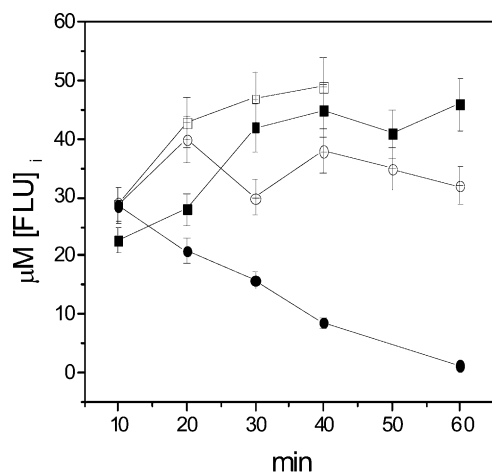


Fig. 5. Efflux of FLU from GLC4/ADR cells. Cells, $10^6/\text{mL}$, were incubated with $20 \mu\text{M}$ DHF-DA for 1 hr. They were then centrifuged and resuspended in DHF-DA free buffer. The intracellular FLU concentration was then determined as a function of time according to the procedure described in Figs. 2 and 3. Cells were GLC4 (■), GSH-depleted GLC4 (□), GLC4/ADR (●) and GSH-depleted GLC4/ADR (○). The values represent mean \pm SD of three independent experiments performed on three different days.

up to $100 \mu\text{M}$ and then plateaued. At the $200 \mu\text{M}$ H_2O_2 concentration used the cells were viable during the short time necessary for the measurement, as checked by trypan blue exclusion.

A third control experiment was made to check the variation of the FLU fluorescence as a function of pH. The fluorescence signal increased from pH 3 up to 7 and then plateaued till pH 10 and then decreased. It follows that, under our experimental conditions, a variation of the FLU fluorescence cannot be due to change in pH (the pH of the cytosol is ~ 7.3 and FLU which is negatively charged cannot accumulated inside intracellular acidic organelles such as lysosomes).

A fourth control was done to check the ATP intracellular level under the different experimental conditions. The ATP concentration was determined using the luciferin–luciferase test [21]. In both cell lines the presence of azide under glucose-free conditions yielded 90% ATP depletion.

3.4. Rate of the MRP1-mediated efflux of FLU and DHF

GLC4 and GLC4/ADR cells were incubated with $20 \mu\text{M}$ DHF-DA. After 1 hr cells were centrifuged and suspended in DHF-DA free buffer. Then after each 10 min aliquot of cells was taken and the signal F_{cyto} was recorded just before and after addition of $200 \mu\text{M}$ H_2O_2 . The calibration curve in Fig. 3 then allowed the determination of $[\text{FLU}]_i$ and $[\text{DHF}]_i$ as a function of time. Figs. 5 and 6 show typical plots of $[\text{FLU}]_i$ and $[\text{DHF}]_i$, respectively, as a function of time for sensitive and resistant cells in normal cells and in GSH-depleted cells.

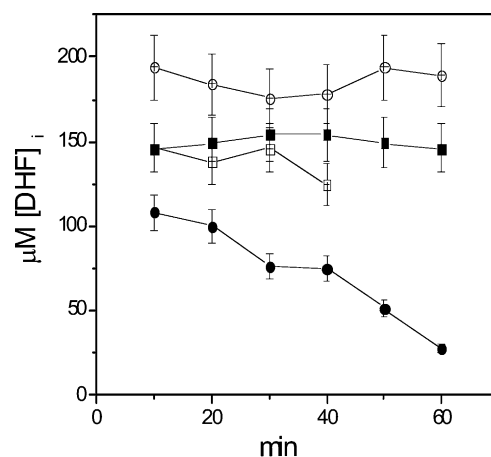


Fig. 6. Efflux of DHF from GLC4/ADR cells. Cells, $10^6/\text{mL}$, were incubated with $20 \mu\text{M}$ DHF-DA for 1 hr. They were then centrifuged and resuspended in DHF-DA free buffer. The intracellular DHF concentration was then determined as a function of time according to the procedure described in Figs. 2 and 3. Cells were GLC4 (■), GSH-depleted GLC4 (□), GLC4/ADR (●) and GSH-depleted GLC4/ADR (○). The values represent mean \pm SD of three independent experiments performed on three different days.

Under these experimental conditions (cells incubated for 1 hr with DHF-DA, then centrifuged and suspended in a free DHF-DA buffer), inside the cells are present DHF-DA, DHF and FLU. The concentration of DHF-DA should decrease because of its cleavage by esterase and the concentration of FLU should increase because of the oxidation of DHF. However, the concentration of DHF can, on the one hand, increase because of the cleavage of DHF-DA and, on the other hand, decrease because of its oxidation to FLU. The observation (Fig. 6) that, in sensitive cells and resistant cells plus BSO, the concentration of DHF remains almost constant strongly suggest that there is a steady state for DHF, i.e. that the rate of cleavage of DHF-DA is very close to the rate of DHF oxidation to FLU. It follows that, in resistant cells, the decrease of the DHF concentration is due to its pumping out by MRP1 only. Our data show that $V_a = (2.5 \pm 0.4) \times 10^{-20}$ mole/cell/s when $[\text{DHF}]_i = 41 \pm 4 \mu\text{M}$ yielding $k_a = (6.1 \pm 1.4) \times 10^{-16}$ L/cell/s ($k_a = V_a/C_i$).

Now let us consider the FLU concentration in sensitive cells and GSH-depleted resistant cells. Here, the concentration of the fluorescent molecule can increase only. Actually, this is what is observed: in Fig. 5 one can see that during the first 30 min, after resuspension of the cells in DHF-DA free buffer, the FLU concentration increases and becomes about 1.5-fold higher than at $t = 0$, and then plateaued. Here, also it follows that the decrease of the FLU concentration in resistant cells is due to its pumping out by MRP1. Our data show that $V_a = (8.8 \pm 1.4) \times 10^{-21}$ mole/cell/s when $[\text{FLU}]_i = 14 \pm 1 \mu\text{M}$ yielding $k_a = (6.3 \pm 1.4) \times 10^{-16}$ L/cell/s ($k_a = V_a/C_i$). Therefore, for these two compounds, the values of the parameters k_a characteristic of the efficiency for the active efflux were very similar.

3.5. Inhibition of the MRP1-mediated efflux of DHF and FLU by PAK-104P and MK571

Resistant cells, $10^6/\text{mL}$, were incubated with $20\text{ }\mu\text{M}$ DHF-DA and either $10\text{ }\mu\text{M}$ PAK-104P or $5\text{ }\mu\text{M}$ MK571. The variation of the intensity of the flow cytometry signal as a function of time was very similar to that observed with sensitive cells indicating that the MRP1-mediated efflux of DHF and FLU was inhibited by these two compounds. Data obtained with PAK-104P are shown in Fig. 2.

4. Discussion

The mechanism by which GSH facilitates transport of some compounds by MRP1 is still a matter of debate. MRP1 is able to transport GSH conjugates, such as dinitrophenyl glutathione and it was found at an early stage that MRP1 was also able to transport non-anionic drugs, such as anthracyclines, vinca alkaloids and epipodophyllotoxins [11–13,19,22]. Attempts to detect derivatives of these drugs conjugated to an anionic ligand (GSH, glucuronic acid, sulphate) have remained unsuccessful and the consensus is now that these drugs are transported as such. So, it seems now recognised that MRP1 can co-transport unmetabolised compounds which are either neutral or cationic [11–13] with GSH. In addition, it has recently been demonstrated that the co-transport of DNR and GSH had a 1:1 stoichiometry [15]. However, the influence of GSH on anionic substrate MRP1-mediated efflux is far from being elucidated [23]. For instance, it has been reported by Feller *et al.* [24] that MRP1 can transport the organic anion calcein without the requirement of GSH, whereas, more recently, Bagrij *et al.* [23] have shown that a decrease of the intracellular GSH concentration lead to a decrease of the MRP1-mediated calcein efflux.

Most of the data found in the literature concerning the MRP1-mediated efflux of compounds are qualitative and it is always difficult to compare the efficiency of the efflux of different substrates by the transporter. For these reasons, for several years we are involved in the quantitative determination of the kinetics parameters because measurement of the kinetic characteristics of substrate transport is a powerful approach for enhancing our understanding of their function and mechanism. For this purpose we use the same cell line throughout our experiments. In most of cases, we characterise this efficiency by calculating the parameter k_a [18–20]. As it is described in the Section 2, k_a is proportional to the ratio V_M/K_m and is very convenient to evaluate the efficiency of a transporter. This parameter is very useful because its value can be estimated from a few number of measurements while the determination of the kinetics parameters V_M and K_m requires (i) a very large number of measurements, (ii) the use of high substrate concentration needed to saturate the transporter and reach the maximal rate. It is not always possible to use such

conditions especially not with living cells. We are aware that k_a , which is proportional to V_M/K_m , contains both the turnover number of the transporter protein (i.e. the number of substrate molecules transported per MRP1 molecule per unit of time) as well as the number of transport proteins in the cell membrane (V_M) and the affinity of the substrate for the transporter (K_m). However, the parameter k_a allows a convenient comparison of the transport efficiency of different substrates in the same cells.

Several dyes deriving from FLU have recently been postulated to be handled by MRP1; indeed, 2',7'-bis(2-carboxyethyl)-5(6)-carboxyfluorescein, used to investigate intracellular pH, and carboxyfluorescein have been shown to be actively effluxed by MRP1-overexpressing cells [25,26]. Such carboxyfluorescein-related compounds appear, therefore, to constitute a new identified class of substrates of MRP1 but, up to now, quantitative data are lacking [27,28].

In this paper, we present data that further characterised the transport of FLU and DHF. The measurement was made in real time using intact cells. The findings presented here are the first to show quantitative information about the kinetics parameters for MRP1-mediated efflux of FLU derivatives in intact cells. The conclusions that emerge from our data are that DHF and FLU are actively pumped, by MRP1, that the active efflux coefficient is very similar for both compounds, and that their efflux is inhibited by typical MRP1 inhibitors, MK571 and PAK-104P [29,30]. Here, it is interesting to compare the values of the k_a parameter for DHF and FLU to those obtained, using the same cell line, for other anionic compounds, such as GSH and calcein, which are MRP1 substrates. We have recently determined that k_a was equal to $(6.3 \pm 2.9) \times 10^{-16}$ and $(4.4 \pm 2.1) \times 10^{-16}$ L/cell/s for calcein and GSH, respectively [14,15], i.e. very close to the values obtained for DHF and FLU (see Table 1). Also it is interesting to remark that, GSH depletion brought about by pretreatment for 24 hr with $25\text{ }\mu\text{M}$ BSO, showed significant effects on efflux of these anionic species. As we have already said, data concerning the effect of GSH on MRP1-mediated efflux of anionic species are conflicting especially those obtained with calcein. Feller *et al.* [24], using GLC4/ADR cells in which the intracellular level is about 14 mM , have observed that a GSH depletion to about 18% of the initial value (i.e. $\sim 2.5\text{ mM}$) has no effect on calcein efflux, whereas, Bagrij *et al.* [23], using COR-L23/R cells, have observed a decrease of calcein efflux when the intracellular level of GSH was decreased to 25% of the initial value, i.e. from ~ 5.1 to 1.1 mM . The different effects observed were, therefore, obtained at different intracellular GSH concentrations. One hypothesis to explain this apparently conflicting data could be that, after BSO treatment, the GSH concentration was sufficient to sustain calcein efflux in GLC4/ADR cells but not in COR-L23/R.

The relative importance of the charge of molecules for their transport by MRP1, can be here considered as the four molecules for which k_a has already been determined, i.e. FLU, DHF, calcein and GSH, have different net negative

Table 1
Rate constant for efflux

Compounds	$k_a = V_M/K_m^a$ (L/cell/s)	Electrostatic charge at pH 7.3	Reference
FLU	$(6.1 \pm 1.4) \times 10^{-16}$	−1	This work
DHF	$(6.3 \pm 1.4) \times 10^{-16}$	−1	This work
GSH	$(4.4 \pm 1.5) \times 10^{-16}$	−1	[11]
Calcein	$(6 \pm 2) \times 10^{-16}$	−5	[10]
Calcein-AM	$(4 \pm 1) \times 10^{-12}$	0	[10]
Daunorubicin	$(1.8 \pm 0.5) \times 10^{-12}$	+1	[15,16]
Tetramethylrosamine	$(0.3 \pm 0.1) \times 10^{-12}$	+1	Unpublished data

^a The data are the means \pm SEM of at least five determinations

charges (Table 1) at pH 7.3. As can be seen, for these molecules, the k_a values are very similar and do not depend on the net negative charge.

It should be also emphasise here that the efficiency of MRP1 to efflux anionic or neutral substrates is about 10^4 -fold lower than its efficiency to pump out neutral or positively charged substrates. For comparison the k_a values previously determined for daunorubicin, calcein-AM and the rhodamine derivative, tetramethylrosamine, are reported in Table 1. The underlying molecular and biochemical causes for the extreme differences in transporter efficiency of the different MRP1 substrates as measured by us, remain unexplained presently.

Acknowledgments

This research was supported by grants from l'Université Paris XIII and CNRS.

References

- [1] Cole SPC, Bhardwaj G, Gerlach JH, Mackie JE, Grant CE, Almquist KC, Stewart AJ, Kurz EU, Duncan AMV, Deeley RG. Overexpression of a transporter gene in a multidrug-resistant human lung cancer cell line. *Science* 1992;258:1650–4.
- [2] Bradley G, Juranka PF, Ling V. Mechanisms of multidrug resistance. *Biochem Biophys Acta* 1988;948:87–128.
- [3] Broxterman HJ, Giaccone G, Lankelma J. Multidrug resistance proteins and other drug transport-related resistance to natural product agents. *Curr Opin Oncol* 1995;7:532–40.
- [4] Higgins CF. ABC transporters—from microorganisms to man. *Annu Rev Cell Biol* 1992;8:67–113.
- [5] Leier I, Jedlitschky G, Buchholz U, Cole SPC, Deeley RG, Keppler D. The MRP gene encodes an ATP-dependent export pump for leukotriene C-4, and structurally related conjugates. *J Biol Chem* 1994;269:27807–10.
- [6] Müller M, Meijer C, Zaman GJR, Borst P, Scheper RJ, Mulder NH, de Vries EGE, Jansen PLM. Overexpression of the gene encoding the multidrug resistance-associated protein results in increased ATP-dependent glutathione S-conjugate transport. *Proc Natl Acad Sci USA* 1994;91:13033–7.
- [7] Broxterman HJ, Schuurhuis GJ, Lankelma J, Oberink JW, Eekman CA, Claessen AME, Hoekman K, Poot M, Pinedo HM. Highly sensitive and specific detection of P-glycoprotein function for hematological and solid tumor cells using a novel nucleic acid stain. *Br J Cancer* 1997;76:1029–34.
- [8] Versantvoort CHM, Broxterman HJ, Bagrij T, Scheper RJ, Twentyman P. Regulation by glutathione of drug transport in multidrug-resistant human lung tumour cell lines overexpressing multidrug resistance-associated protein. *Br J Cancer* 1995;72:82–9.
- [9] Hollo Z, Homolova L, Hegedus T, Sarkadi B. Transport properties of the multidrug resistance-associated protein (MRP) in human tumour cells. *FEBS Lett* 1996;383:99–104.
- [10] Deeley RG, Cole SPC. Function evolution and structure of multidrug resistance protein (MRP). *Semin Cancer Biol* 1997;8:193–204.
- [11] Loe DW, Almquist KC, Deeley RG, Cole SPC. Multidrug resistance protein (MRP)-mediated transport of leukotriene C-4 and chemotherapeutic agents in membrane vesicles—demonstration of glutathione-dependent vincristine transport. *J Biol Chem* 1996;271:9675–82.
- [12] Rappa G, Lorico A, Flavell RA, Sartorelli AC. Evidence that the multidrug resistance protein MRP functions as a co-transporter of glutathione and natural produce toxins. *Cancer Res* 1997;57:15232–7.
- [13] Renes J, De Vries EGE, Nuenhuis EF, Jansen PLM, Müller M. ATP- and glutathione-dependent transport of chemotherapeutic drugs by the multidrug resistance protein MRP1. *Br J Pharmacol* 1999;126:681–8.
- [14] Essodaigui M, Broxterman HJ, Garnier-Suillerot A. Kinetic analysis of calcein and calcein-acetoxymethylester efflux mediated by the multidrug resistance protein and P-glycoprotein. *Biochemistry* 1998;37:2243–50.
- [15] Salerno M, Garnier-Suillerot A. Kinetics of glutathione and daunorubicin efflux from multidrug resistance protein overexpressing small-cell lung cancer cells. *Eur J Pharmacol* 2001;421:1–9.
- [16] Zijlstra JG, De Vries EGE, Mulder NH. Multifactorial drug resistance in an adriamycin-resistant human small cell lung carcinoma cell line. *Cancer Res* 1987;47:1780–4.
- [17] Fernandez-Checa JC, Kaplowitz N. The use of monochlorobimane to determine hepatic GSH levels and synthesis. *Anal Biochem* 1990;190:212–9.
- [18] Mankhetkorn S, Dubru F, Hesschenbrouck J, Fiallo M, Garnier-Suillerot A. Relation among the resistance factor kinetics of uptake, and kinetics of the P-glycoprotein-mediated efflux of doxorubicin, daunorubicin, 8-(S)-fluoroidarubicin, and idarubicin in multidrug-resistant K562 cells. *Mol Pharmacol* 1996;49:532–9.
- [19] Marbeuf-Gueye C, Broxterman HJ, Dubru F, Priebe W, Garnier-Suillerot A. Kinetics of anthracycline efflux from multidrug resistance protein-expressing cancer cells compared with P-glycoprotein-expressing cancer cells. *Mol Pharmacol* 1998;53:141–7.
- [20] Marbeuf-Gueye C, Ettori E, Priebe W, Kozlowski H, Garnier-Suillerot A. Correlation between the kinetics of anthracycline uptake and the resistance factor in cancer cells expressing the multidrug resistance protein or the P-glycoprotein. *Biochim Biophys Acta* 1999;1450:374–84.
- [21] Kimmich G, Randles J, Brand J. Assay of picomole amounts of ATP, ADP and AMP using the luciferase enzyme system. *Anal Biochem* 1975;69:187–91.
- [22] Zaman GJR, Flens MJ, Van Leusden MR, De Haas M, Mulder HS, Lankelma J, Pinedo HM, Scheper RJ, Baas F, Broxterman HJ, Borst P. The human multidrug resistance-associated protein MRP is a plasma membrane drug-efflux pump. *Proc Natl Acad Sci USA* 1994;91:8822–6.

- [23] Bagrij T, Klokouzas A, Hladky SB, Barrand MA. Influences of glutathione on anionic substrate efflux in tumour cells expressing the multidrug resistance-associated protein, MRP1. *Biochem Pharmacol* 2001;62:199–206.
- [24] Feller N, Broxterman HJ, Wahrer DC, Pinedo HM. ATP-dependent efflux of calcein by the multidrug resistance protein (MRP): no inhibition by intracellular glutathione depletion. *FEBS Lett* 1995;368:385–8.
- [25] Draper MP, Martell RL, Levy SB. Active efflux of the free acid form of the fluorescent dye 2',7'-bis(2-carboxyethyl)-5(6)-carboxyfluorescein in multidrug-resistance-protein-overexpressing murine and human leukemia cells. *Eur J Biochem* 1997;243:219–24.
- [26] Van der Kolk DM, De Vries EG, Koning JA, van den Berg E, Muller M, Vellenga E. Activity and expression of the multidrug resistance proteins MRP1 and MRP2 in acute myeloid leukemia cells tumor cell lines and normal hematopoietic CD34⁺ peripheral blood cells. *Clin Cancer Res* 1998;4:1727–36.
- [27] Laupeze B, Amiot L, Courtois A, Vernhet L, Drenou B, Fauchet R, Fardel O. Use of the anionic dye carboxy-2',7'-dichlorofluorescein for sensitive flow cytometric detection of multidrug resistance-associated protein activity. *Int J Oncol* 1999;15:571–6.
- [28] Sun H, Johnson DR, Finch RA, Sartorelli AC, Miller DW, Elmquist WF. Transport of fluorescein in MDCKII-MRP1 transfected cells and mrp1-knockout mice. *Biochem Biophys Res Commun* 2001;284: 863–9.
- [29] Leier I, Jedlitschky G, Buchholz U, Center M, Cole SPC, Deeley RG, Keppler D. ATP-dependent glutathione disulphide transport mediated by the MRP gene-encoded conjugate export pump. *Biochem J* 1996; 314:433–7.
- [30] Marbeuf-Gueye C, Salerno M, Quidu P, Garnier-Suillerot A. Inhibition of the P-glycoprotein-and multidrug resistance protein-mediated efflux of anthracyclines and calceinacetoxymethyl ester by PAK-104P. *Eur J Pharmacol* 2000;391:207–16.